Drugs R D (2014) 14:333–340
DOI 10.1007/s40268-014-0074-4

ORIGINAL RESEARCH ARTICLE

C_{60} Fullerene as Synergistic Agent in Tumor-Inhibitory Doxorubicin Treatment

Svitlana Prylutska · Iryna Grynyuk · Olga Matyshevska · Yuriy Prylutskyy · Maxim Evstigneev · Peter Scharff · Uwe Ritter

Published online: 12 December 2014
© The Author(s) 2014. This article is published with open access at Springerlink.com

Abstract

Background Doxorubicin (Dox) is one of the most potent anticancer drugs, but its successful use is hampered by high toxicity caused mainly by generation of reactive oxygen species. One approach to protect against Dox-dependent chemical insult is combined use of the cytostatic drug with antioxidants. C_{60} fullerene has a nanostructure with both antioxidant and antitumor potential and may be useful in modulating cell responses to Dox.

Objective The aim of this study was to estimate the antitumor effect and antioxidant enzyme activity of combined C_{60} fullerene and Dox (C_{60} + Dox) in the liver and heart of mice with Lewis lung carcinoma compared with Dox treatment alone.

Methods Highly stable pristine C_{60} fullerene aqueous colloid solution (concentration 1.0 mg/ml, average hydrodynamic diameter of nanoparticles 50 nm) was used in the study and characterized by means of atomic force microscopy (AFM). The in vivo investigation of C_{60}-Dox action was performed via the standard methods of histological and enzyme activity analyses.

Results Dox (total dose 2.5 mg/kg) combined with C_{60} fullerene (total dose 25 mg/kg) in tumor-bearing animals resulted in tumor growth inhibition, prolongation of life, metastasis inhibition, and increased number of apoptotic tumor cells and was more effective than the corresponding course of Dox treatment alone. C_{60} fullerene demonstrated a protective effect against superoxide dismutase and glutathione peroxidase inhibition induced by Dox-dependent oxidative insult in the liver and heart.

Conclusion Combined treatment with C_{60} + Dox is considered to be a promising approach for cancer chemotherapy.

Key Points

C_{60} fullerene protects the heart and liver of tumor-bearing animals against doxorubicin (Dox)-induced oxidative stress.

Combined antitumor treatment of C_{60} fullerene and Dox is more effective than Dox treatment alone.

S. Prylutska · I. Grynyuk · O. Matyshevska · Y. Prylutskyy (✉) · P. Scharff · U. Ritter
Joint Ukrainian-German Center on Nanobiotechnology, Kyiv, Ukraine
e-mail: prylut@ukr.net

S. Prylutska · I. Grynyuk · O. Matyshevska · Y. Prylutskyy
Taras Shevchenko National University of Kyiv, Volodymyrska Str., 64, Kyiv 01601, Ukraine

M. Evstigneev (✉)
Department of Biology and Chemistry, Belgorod State University, 85 Pobedy Str., Belgorod 308015, Russia
e-mail: max_evstigneev@mail.ru

P. Scharff · U. Ritter
Institute of Chemistry and Biotechnology, Technical University of Ilmenau, Weimarer Str. 25, Ilmenau 098693, Germany

1 Introduction

Oncological diseases, particularly lung cancer, breast cancer, and leucosis, are common and carry a high mortality rate. Several cytostatic drugs, including doxorubicin (Dox), are used in the therapy of malignant tumors. Dox is an antibiotic of the anthracycline group, with a wide range of

clinical activity against solid tumors and hemoblastoses, lung carcinoma, and acute leukemia [1]. Dox non-covalently binds to DNA, blocking the synthesis of nucleic acids, and demonstrates high antimitotic activity and pronounced mutagenic effect, but exerts toxic effects in normal tissues and cells [2].

One approach to protect against Dox-induced chemical insult to normal tissues is a combined use of the cytostatic drug with antioxidants of a different nature [3]. C_{60} fullerene has recently been recognized as a promising agent for use in anticancer therapy [4, 5]. C_{60} fullerene and its derivatives are biocompatible, show no toxic effects on normal tissues at low concentrations, possess strong free-radical-scavenging and antioxidant potential [6–10], and demonstrate a protective effect against Dox-induced chronic cardio- and hepatotoxicity [11]. The tumor-inhibitory activity of nanoparticles containing C_{60} fullerene has been studied in models of murine hepatocarcinoma [12] and rat colorectal cancer and mammary carcinoma [3, 13, 14]. Finally, recent results indicate that C_{60} fullerene complexation with Dox may be a key process leading to alteration of the antitumor effect of Dox in vitro [15, 16].

The study of the biological effects of pristine C_{60} fullerene is limited by its hydrophobicity, difficulties involved with reaching sufficient concentration, and aggregation in water [17]. For this reason, hydrophilic derivatives obtained by chemical modification of the C_{60} fullerene outer surface were used in most studies of C_{60} fullerene antioxidant and antineoplastic effects [10, 12, 18]. However, derivatization does not completely prevent cluster formation. Moreover, substantial modification of the C_{60} fullerene core appears to cause a perturbation of the π-conjugated electronic system of cyclohexatriene units on the molecular surface and hence may influence C_{60} fullerene reactivity [19, 20]. The use of a stable water colloid dispersion of pristine C_{60} fullerene has shown promise for the comprehensive analysis of C_{60} fullerene biological effects and antitumor efficiency [21].

The aim of this study was to estimate the antitumor effect and antioxidant enzyme activity in the liver and heart of mice with Lewis lung carcinoma (LLC) after combined treatment with C_{60} fullerene and Dox as compared with treatment with Dox alone.

2 Materials and Methods

2.1 Chemicals

Dox (Ebewe, Austria), paraformaldehyde, paraplast (Richard-Allan Scientific, USA), DC Protein (Bio-Rad, USA), superoxide dismutase (SOD), and glutathione peroxidase (GP) assay kits were purchased from Fluka (Buchs, Switzerland) and Sigma-Aldrich (Saint Louis, USA).

2.2 Preparation of Pristine C_{60} Fullerene Water Colloid Solution

The C_{60} fullerene powder with a purity of >99.8 % was prepared according to a published protocol [22]. The highly stable and reproducible pristine C_{60} fullerene aqueous colloid solution (C_{60}FAS; concentration 1.0 mg/ml, purity >99.5 %) was prepared, as published previously [23], by the transfer of C_{60} fullerene molecules from toluene to an aqueous phase with the help of ultrasonic treatment.

2.3 Atomic Force Microscopy Characterization of C_{60} Fullerene Aqueous Colloid Solution

The state of C_{60} fullerene in aqueous solution was monitored using atomic force microscopy (AFM; 'Solver Pro M' system; NT-MDT, Russia). The samples were deposited by precipitation from an aqueous solution droplet onto cleaved mica substrate (V-1 Grade, SPI Supplies). Measurements were performed after complete evaporation of the solvent. The sample visualization was carried out in semicontact (tapping) mode with NSG10 (NT-MDT) probes.

2.4 Animals

Male C57Bl/6J mice (20–22 g) were kept at 20 ± 1 °C with free access to standard laboratory diet and water. All experiments were performed according to the international principles of the European Convention on protection of vertebrate animals used for experimental purposes.

2.5 Treatment Protocol

LLC cells ($\sim 5 \times 10^5$) were subcutaneously inoculated into the limb of each mouse. The treatment was started on the 7th day after tumor inoculation when the tumor had grown up to approximately 5 mm. Tumor-bearing mice were randomly divided into four groups, with 12 animals per group.

Mice in the Dox group and the C_{60} fullerene group received intraperitoneal (ip) injection of 0.5 mg/kg of Dox and 5 mg/kg of C_{60} fullerene, respectively, as a daily dose for 5 consecutive days with a 1-day interval [4]. Mice in the C_{60} + Dox group received C_{60}FAS ip (dose 5 mg/kg) 20 min before the Dox injection (dose 0.5 mg/kg). The control cancer group received saline ip only. On the 22nd day after tumor inoculation (when the first tumor-bearing animal died in the control cancer group), each group was randomly divided into two groups; six mice from each

group were sacrificed and tissues were taken for analysis. The remaining six mice in each group were used to estimate the lifespan.

2.6 Assay of Antitumor Effects

The antitumor efficiency of the applied technique was estimated with the following quantitative indexes:

- tumor volume: $V = \frac{ab^2}{2}$, where a and b are the long and short diameter of the tumor (mm), respectively [12];
- prolongation of animal life: $k_p = \frac{t_e - t_c}{t_c} \times 100\ \%$, where t_c and t_e are the average lifespan (in days) in cancer control (c) and experimental (e) groups of animals, respectively [4];
- metastasis inhibition: $k_m = \frac{A_c \times B_c - A_e \times B_e}{A_c \times B_c} \times 100\ \%$, where A_c and A_e are the frequency of tumor cell colonies that have metastasized to the lung; B_c and B_e are the average number of metastases in the lung of animals in the cancer control (c) and experimental (e) groups, respectively [4].

2.7 Histological Studies

For histological analysis, tumor tissue was dissected, fixed in 4 % paraformaldehyde, pH 7.4, dehydrated in ethanol, embedded at paraplast, and cut into 4 μm slices. After staining with hematoxylin-eosin (HE), cyto-morphological characteristics of tumor sections were studied using light microscopy (Olympus BX51, Japan). The average number of mitotic (with the specific pattern of chromatin condensation) and apoptotic (with fragmented nucleus and apoptotic bodies) cells was estimated in sections with the use of 'Olympus DP-Soft' morphometric software.

Mitotic or apoptotic indexes were estimated with the following formula: $I = \frac{NC}{TNC} \times 100\ \%$, where NC is the number of mitotic or apoptotic cells, and TNC is the total number of cells.

2.8 Measurement of Antioxidant Enzyme Activity

The liver and heart were quickly removed from the scarified mice, placed into an ice-cold solution, minced, and homogenized in 10 mM Tris–HCl, pH 8.0. The samples were centrifuged at 13,000g for 20 min at 4 °C. Supernatants were used for the assay of total protein concentration and spectrophotometric analysis of enzyme activity. Protein concentration was determined using a DC Protein Assay Kit.

SOD activity was measured using a competition assay between SOD and indicator molecule, nitroblue tetrazolium (NBT). One unit of activity was defined as the concentration of SOD that had inhibited the NBT reduction rate to half of the maximum. GP activity was estimated in potassium buffer containing reduced glutathione, NaN_3, to inhibit catalase and H_2O_2 as the substrate by monitoring accumulation of glutathione disulfide (GSSG).

2.9 Statistics

Statistical analysis of experimental data was performed using the Statistica-6.0 computer program (StatSoft Inc.). Validity of differences between the control and experimental measurements was estimated via the Student's t-test (values are given as mean ± standard error; the differences between the compared values were considered meaningful at $p < 0.05$).

3 Results and Discussion

3.1 Structure of C_{60} Fullerene Nanoparticles in Aqueous Colloid Solution

Knowledge of the C_{60} fullerene aggregation parameters in aqueous solution is important for estimation of nanostructure bioactivity and its potential for biomedical application [18, 24, 25]. An AFM investigation was performed to characterize the aggregation state of C_{60} fullerene in aqueous solution.

The AFM image (Fig. 1) demonstrates that, along with the individual C_{60} fullerenes, their bulk aggregates (clusters) with a diameter of up to 50 nm were present on the mica substrate. These results are in a good agreement with the data from laser correlation spectroscopy of C_{60}FAS, which confirm that the average hydrodynamic diameter of nanoparticles is 50 nm and no further agglomeration is observed [26]. More detailed analysis of the structural composition and physico-chemical properties of C_{60}FAS has been previously accomplished [21, 23] by means of chemical analysis, ultraviolet-visible spectroscopy (UV/VIS) and Fourier transform infrared spectroscopy (FTIR), scanning tunneling microscopy, dynamic light scattering, and small-angle neutron scattering techniques. In general, the properties of the C_{60}FAS used in this experiment correspond to those in the published literature data.

3.2 Tumor Growth-Inhibitory Effects

In traditional animal tumor models, Dox is typically introduced at concentrations of up to 100 mg/kg; however, high lethality complicates prolonged monitoring of Dox effects. Injection of the chemotherapeutic agent in lower doses is more effective than a single injection at an equivalent dose [2].

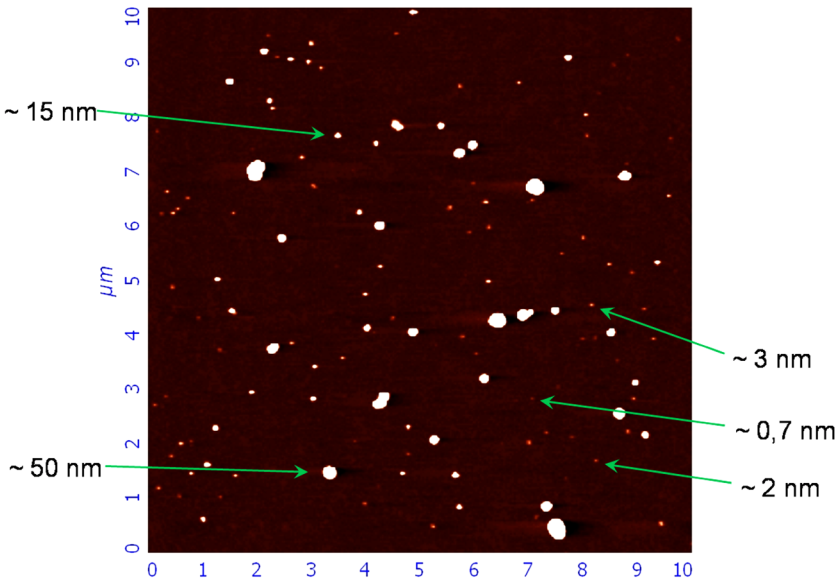

Fig. 1 Atomic force microscopy image of C_{60} fullerene nanoparticles precipitated on mica surface from C_{60}FAS (0.1 mg/ml)

In our experiments, we used a model of multiple ip injections for a course of Dox treatment with a total dose of 2.5 mg/kg (corresponding to a minimal therapeutic dose), and in combination with C_{60} fullerene as a potential antitumor agent and protector against Dox-induced toxicity. The total dose of C_{60} fullerene (25 mg/kg) was non-toxic as expected, since the median lethal dose (LD_{50}) for pristine C_{60} fullerene ip injected in a water solution to mice was found to be approximately 600 mg/kg [6].

The kinetics of average tumor volume extension that manifests the tumor growth was measured in three experimental groups of animals from the 7th to 22nd day after tumor inoculation and compared with that of the control cancer group. The tumor growth inhibition curves for the various groups are shown in Fig. 2. The tumors grew the quickest in the control group. Tumor inhibitory effect in the C_{60} fullerene-treated group (22.5 %) was comparable with that in the Dox-treated group (24.2 %). When C_{60} fullerene was administered before Dox (C_{60} + Dox group), a stronger inhibitory effect was observed (36.2 %). Thus, these data indicate that treatment with C_{60} + Dox more effectively inhibits tumor growth than does treatment with Dox or C_{60} fullerene separately.

3.3 Quantitative Indexes of Antitumor Effect

Data on the lifespan of the control and treated groups are presented in Table 1. The last animal in the control cancer group died on the 30th day of the experiment, whereas the lifespan of animals in experimental groups was found to be increased. The last animal in the Dox group died on the 38th day, and those in the C_{60} fullerene and C_{60} + Dox groups died on the 40th day.

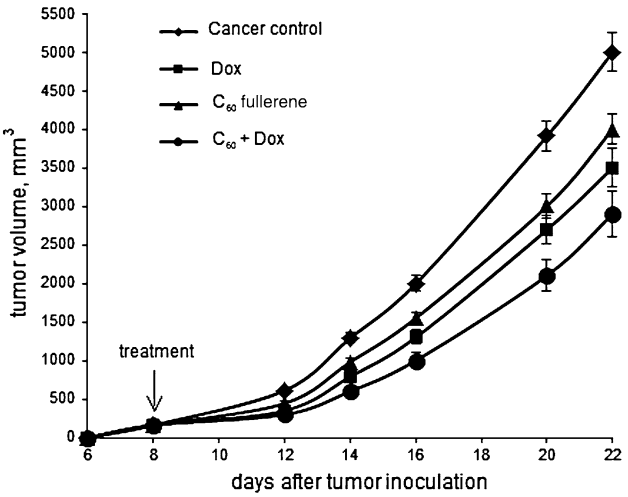

Fig. 2 Growth inhibition curves for treatment of tumor-bearing animals with C_{60} fullerene, doxorubicin, or C_{60} + doxorubicin ($p < 0.05$)

Table 2 shows the quantitative indexes of animal life prolongation (k_p) and metastasis inhibition (k_m) as the measure of the total effectiveness of the applied regimes of antitumor treatment.

LLC cells are highly invasive and quickly spread into lung tissue and form multiple metastases. Dox treatment distinctly inhibited tumor dissemination into the lung of tumor-bearing animals ($k_m \sim 23$ %) but exerted only a slight effect on life prolongation ($k_p \sim 16$ %). In the C_{60} fullerene-treated group, the metastasis inhibition index was less than that in the Dox-treated group ($k_m \sim 15$ %), but the life prolongation was greater ($k_p \sim 24$ %). Both the anti-metastatic effect ($k_m \sim 35$ %) and the life prolongation ($k_p \sim 32$ %) were found to be maximal in the C_{60} + Dox group.

Table 1 Lifespan of animals in different groups

Days after tumor inoculation	Treatment group (n)			
	Cancer control	Doxorubicin	C_{60} fullerene	C_{60} + doxorubicin
22	6	6	6	6
24	2	5	5	5
26	1	2	4	
28			3	
30	0			3
32			2	
34		1		
36			1	
38		0		1
40			0	0

Table 2 Indexes of metastasis inhibition (k_m) and animal life prolongation (k_p) in groups of treated tumor-bearing mice

Treatment	k_m, %	k_p, %
Doxorubicin	23 ± 4*	16 ± 4
C_{60} fullerene	15 ± 2	24 ± 4*
C_{60} + doxorubicin	35 ± 5*	32 ± 5*

* $p < 0.05$ compared with the cancer control group (untreated animals)

3.4 Cytomorphological Changes in Tumor Tissue

Cytomorphological study of the tumor that developed subcutaneously in mice in the cancer control group (Fig. 3a) showed that it consisted of polymorphic cells with a nucleus, large nucleolus, condensed chromatin, and light areas of tumor karyoplasm. The high content of mitotic cells testifies to the proliferative potential of tumor cells. In the C_{60} fullerene-treated group, the tumor mitotic index did not change, but the apoptotic index was found to be higher than in the control cancer group (Figs. 3b and 4). Dox treatment was followed by a reduction in the number of mitotic cells and an increase in the number of apoptotic cells, i.e. by inhibition of proliferative potential and induction of tumor cell death (Figs. 3c, 4). When the tumor-bearing animals were exposed to treatment with C_{60} + Dox, the number of apoptotic cells substantially increased and zones containing apoptotic, necrotic cells and infiltrating macrophages were detected (Figs. 3d and 4).

3.5 Activity of Antioxidant Enzymes in Liver and Heart

Dox chemotherapy is known to be accompanied by the generation of reactive oxygen species (ROS) and immediate oxidative damage of cells with high oxidative metabolism and activity of mitochondrial respiratory chain, particularly cardiac myocytes and hepatocytes. SOD and GP are the predominant antioxidant enzymes. The first step of antioxidant defense is the dismutation of superoxide anion into hydrogen peroxide by inducible SOD; the second is conversion of hydrogen peroxide to water by GP. The activity of SOD and GP was estimated in the liver and heart of animals in the cancer control, Dox-, and C_{60} + Dox-treated groups. No reliable difference in the level of heart and liver antioxidant enzymes in the C_{60} fullerene group as compared with the cancer control group was observed.

Prolonged Dox administration resulted in a decrease of SOD as well as of GP activities in both mice liver and mice heart (Fig. 5). Since activity of both enzymes is known to undergo feedback inhibition by excessive levels of peroxides and lipoperoxides, it could be that Dox-dependent oxidative stress diminishes ROS-scavenging activity of SOD and GP in the liver and heart of tumor-bearing animals.

No inhibition of antioxidant enzyme activity was detected in the C_{60} + Dox-treated group; the level became comparable with that in the control group (SOD activity in liver and heart and GP activity in heart) or even exceeded that in the control group (GP in liver) (Fig. 5). This favorable phenomenon is likely to be associated with the ability of C_{60} fullerene to function as a ROS scavenger or SOD mimetic [27] and to decrease the production of ROS to the optimal level for antioxidant enzyme activation. Up-regulation of SOD has previously been shown to enhance cell survival in the presence of Dox through its role as a free radical scavenger [28]. In addition, overexpression of cytosolic and mitochondrial GP appeared to protect mice hearts against Dox-induced cardiotoxicity and to prevent impairment of mitochondrial respiration and inhibition of complex I activity [29].

This study has shown that the treatment of tumor-bearing mice with ip injection of C_{60} + Dox from the 7th day after LLC cell inoculation resulted in tumor growth slowdown, metastasis inhibition, and lifespan prolongation. These indexes were also increased after Dox or C_{60} fullerene were administered as single agents, but the antitumor effect was most pronounced in the C_{60} + Dox group. The histological analysis of tumor tissue in the C_{60} + Dox-treated group confirmed the inhibition of proliferating tumor cells, induction of apoptotic and necrotic cell death, and macrophage infiltration.

In several previous in vitro studies, internalization of pristine C_{60} fullerene into cancer cells was demonstrated, but no cytotoxic effects were observed. When human lung carcinoma A549 cells were exposed to pristine C_{60} fullerene dispersion (particle size 100–200 nm), internalized

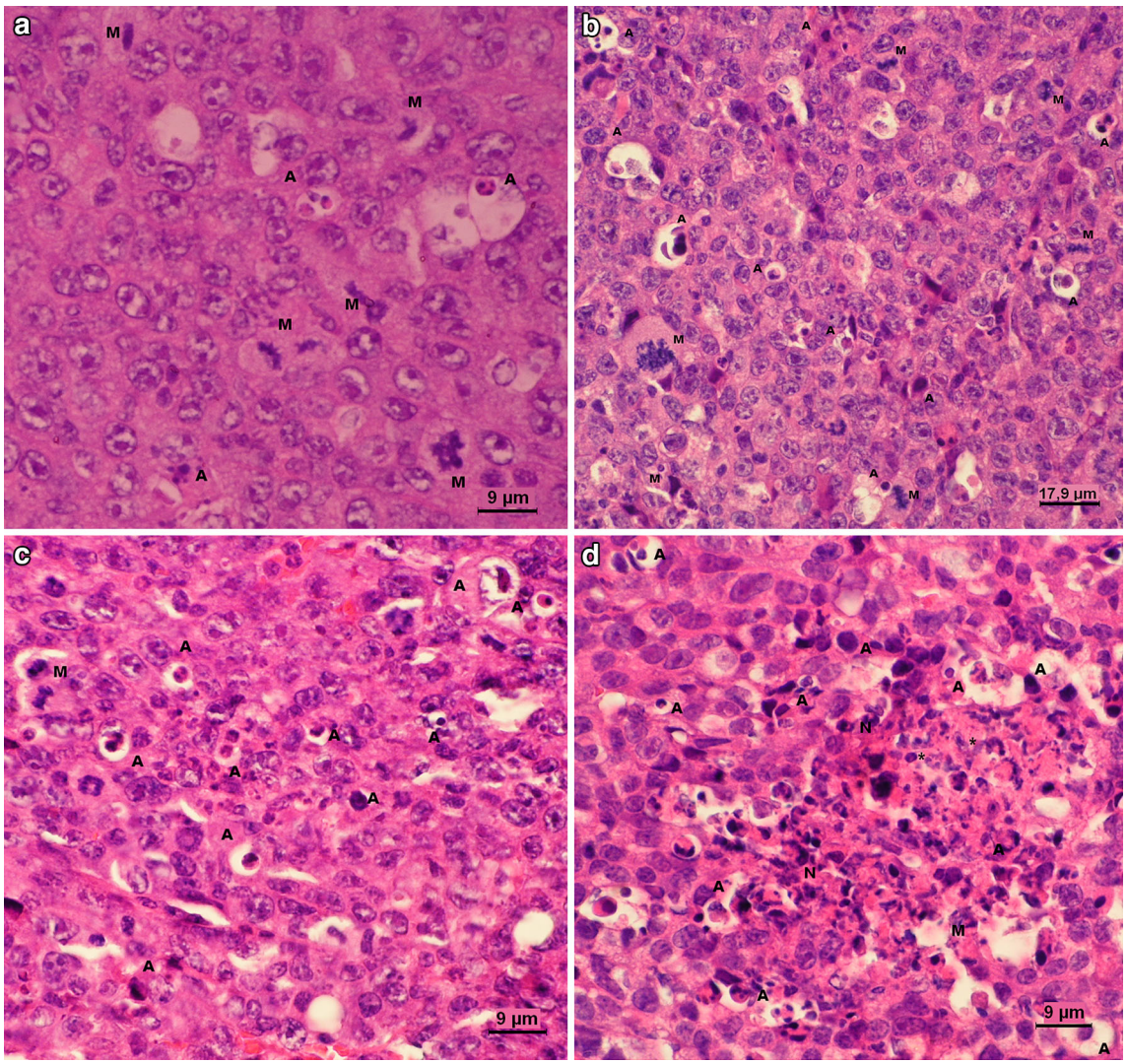

Fig. 3 Histological sections of hematoxylin–eosin-stained tumor tissue (magnification × 400): (**a**) cancer control group, (**b**) C_{60} fullerene group, (**c**) doxorubicin group, (**d**) C_{60} + doxorubicin group. *A* apoptosis, *M* mitosis, *N* necrosis, *indicates macrophage

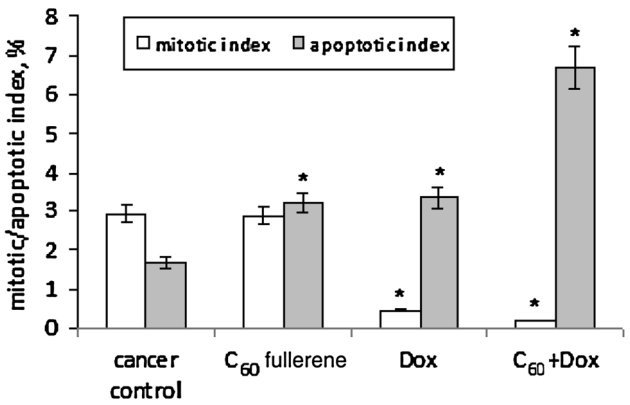

Fig. 4 Tumor mitotic and apoptotic indexes in groups of treated tumor-bearing mice. *$p < 0.05$ vs. the cancer control group (untreated animals). *C_{60}* C_{60} fullerene, *Dox* doxorubicin

C_{60} fullerene aggregates were detected in the cytoplasm and lysosomes. Neither apoptosis nor necrosis was induced, while cell proliferation was inhibited [30]. Malignant breast epithelial cells were shown to take up pristine C_{60} fullerene from methanol C_{60} fullerene solution (particle size 106–342 nm), and the treatment of these cells with C_{60} fullerene up to 200 μg/ml did not alter the morphology, cytoskeleton organization, cell cycle dynamics, or cell proliferation [31].

Other studies on pristine C_{60} fullerene distribution in animal tissues after ip administration demonstrated nanoparticle uptake into the circulation, accumulation in the liver at 120 min post-exposure, and nearly complete elimination by day 13, with minimal accumulation in the spleen, lung, and muscle [6, 32].

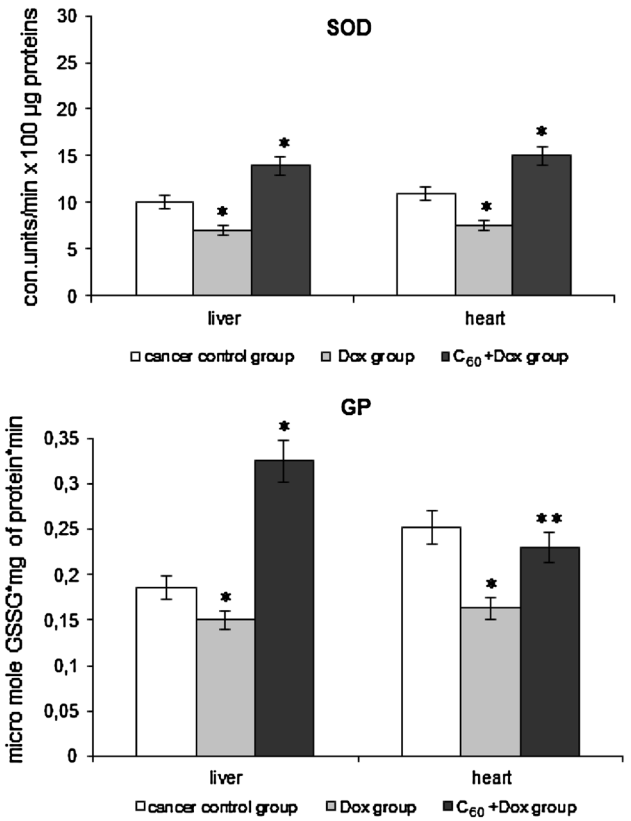

Fig. 5 Activity of superoxide dismutase and glutathione peroxidase in the livers and hearts of treated tumor-bearing mice. $*p < 0.05$ vs. the cancer control group (untreated animals), $**p < 0.05$ vs. the doxorubicin group. *C60* C_{60} fullerene, *Dox* doxorubicin, *GP* glutathione peroxidase, *SOD* superoxide dismutase

Internalization of C_{60} fullerene in tumor tissue has also been demonstrated with in vivo models and different water-soluble C_{60} fullerene derivatives. In a mouse model of liver cancer, malonodiserinolamide-derivatized C_{60} fullerene nanoparticles were detected permeating through the altered vasculature of the tumor, evading the reticulo-endothelial system [33]. $Gd@C_{82}(OH)_{22}$ nanoparticles administered ip at a dose level of approximately 10^{-7} mol/kg were shown to exhibit high antineoplastic activity against murine H22 hepatocarcinoma, but only 0.05 % of the exposed dose reached the tumor tissue [34]. It was also demonstrated that fullerol $C_{60}(OH)_x$ nanoparticles were mainly taken up by the mononuclear phagocyte system, and only 0.2 % were accumulated in the murine H22 hepatocarcinoma within 24 h due to enhanced permeability and retention effects [35]. Nevertheless, $C_{60}(OH)_x$ in doses of 0.2 and 1 mg/kg was found to exhibit significant tumor-inhibitory activity [12].

Considering that no marked accumulation of C_{60} fullerene was detected in tumors and no direct toxic effect on tumor cells was observed, it is assumed that antitumor efficiency of C_{60} fullerene derivatives is not due to the direct killing of tumor cells but is the result of tumor microenvironment regulation and/or immune response activation [12, 36–38]. On the other hand, our finding of C_{60} fullerene-dependent enhancement of Dox antitumor effect does not exclude the possibility that C_{60} fullerene nanoparticles promote Dox accumulation in tumor cells by activating drug endocytosis, as it was shown for $Gd@C_{82}(OH)_{22}$ nanoparticles that may restore defective endocytosis of cisplatin by cancer cells [39].

The most severe side effect of Dox treatment is free radical-mediated damage to liver and heart tissue, which are very sensitive to free radical damage because of their high oxidative metabolism. In this study, we have demonstrated a beneficial effect of pristine C_{60} fullerene in a low-dose regime (5 mg/kg) on heart and liver antioxidant defense against Dox treatment in tumor-bearing mice. The greater protective effect of lower doses of fullerols (25 mg/kg) in contrast to higher doses (50 and 100 mg/kg) against Dox-associated toxicity was confirmed for rat hearts and livers with colorectal cancer [3, 40]. This observation is likely to be associated with the fact that the higher doses were less well absorbed from the peritoneal cavity.

In summary, we can conclude that pristine C_{60} fullerene exhibits health effects and antitumor activity in combined treatment with Dox. These results need to be investigated further in a number of tumor models.

Acknowledgments This work was partially supported by DAAD (S. Prylutska) and the Russian Science Fund (Project N14-14-00328).

Conflict of interests The authors declare no conflicts of interest.

Author contributions Professors M. Evstigneev and P. Scharff, and Dr. U. Ritter were responsible for synthesizing and characterizing the nanomaterials. Professors O. Matyshevska and Y. Prylutskyy carried out the in vivo experiments. Drs. S. Prylutska and I. Grynyuk were responsible for measurement of antioxidant enzyme activity and histological studies.

Open Access This article is distributed under the terms of the Creative Commons Attribution Noncommercial License which permits any noncommercial use, distribution, and reproduction in any medium, provided the original author(s) and the source are credited.

References

1. De Vita VT, Hellman S, Rosenberg SA. Principles and practice of oncology. 6th ed. Philadelphia: Lippincott Williams and Wilkins; 2001. p. 1126–61.
2. Menna P, Paz OG, Chello M, Covino E, Salvatorelli E, Minotti G. Anthracycline cardiotoxicity. Expert Opin Drug Saf. 2012;11:21–36.
3. Injac R, Perse M, Cerne M, Potocnik N, Radic N, Govedarica B, Djordjevic A, Cerar A, Strukelj B. Protective effects of fullerenol $C_{60}(OH)_{24}$ against doxorubicin-induced cardiotoxicity and hepatotoxicity in rats with colorectal cancer. Biomaterials. 2009;30:1184–96.
4. Prylutska SV, Burlaka AP, Klymenko PP, Grynyuk II, Prylutskyy YuI, Schuetze Ch, Ritter U. Using water-soluble C_{60} fullerenes in anticancer therapy. Cancer Nanotechnol. 2011;2:105–10.

5. Prylutska SV, Burlaka AP, Prylutskyy YuI, Ritter U, Scharff P. Pristine C_{60} fullerenes inhibit the rate of tumor growth and metastasis. Exp Oncol. 2011;33:162–4.
6. Gharbi N, Pressac M, Hadchouel M, Szwarc H, Wilson S, Moussa F. [60] Fullerene is a powerful antioxidant in vivo with no acute or subacute toxicity. Nano Lett. 2005;5:2578–85.
7. Kolosnjaj J, Szwarc H, Moussa F. Toxicity studies of fullerenes and derivatives. Adv Exp Med Biol. 2007;620:168–80.
8. Prylutska SV, Grynyuk II, Matyshevska OP, Prylutskyy YI, Ritter U, Scharff P. Anti-oxidant properties of C_{60} fullerenes in vitro. Fuller Nanotub Carbon Nanostruct. 2008;5–6:698–705.
9. Johnston HJ, Hutchison GR, Christensen FM, Aschberger K, Stone V. The biological mechanisms and physicochemical characteristics responsible for driving fullerene toxicity. Toxicol Sci. 2010;114:162–82.
10. Trpkovic A, Todorovic-Markovic B, Trajkovic V. Toxicity of pristine versus functionalized fullerenes: mechanisms of cell damage and the role of oxidative stress. Arch Toxicol. 2012;86:1809–27.
11. Injac R, Radic N, Govedarica B, Perse M, Cerar A, Djordjevic A, Strukelj B. Acute doxorubicin pulmotoxicity in rats with malignant neoplasm is effectively treated with fullerenol $C_{60}(OH)_{24}$ through inhibition of oxidative stress. Pharmacol Rep. 2009;61:335–42.
12. Zhu J, Ji Z, Wang J, Sun R, Zhang X, Gao Y, Sun H, Liu Y, Wang Z, Li A, Ma J, Wang T, Jia G, Gu Y. Tumor-inhibitory effect and immunomodulatory activity of fullerol $C_{60}(OH)_x$. Small. 2008;4:1168–75.
13. Injac R, Perse M, Obermajer N, Djordjevic-Milic V, Prijatelj M, Djordjevic A, Cerar A, Strukelj B. Potential hepatoprotective effects of fullerenol $C_{60}(OH)_{24}$ in doxorubicin-induced hepatotoxicity in rats with mammary carcinomas. Biomaterials. 2008;24–25:3451–60.
14. Perše M, Injac R, Djordjevic A, Štrukelj B. Protective effect of fullerenol on colon cancer development in dimethylhydrazine rat model. Digest J Nanomater Biostruct. 2011;6:1543–51.
15. Skamrova GB, Laponogov I, Buchelnikov AS, Shckorbatov YG, Prylutska SV, Ritter U, Prylutskyy YuI, Evstigneev MP, Ritter U. Interceptor effect of C_{60} fullerene on the in vitro action of aromatic drug molecules. Eur Biophys J. 2014;43:265–76.
16. Prylutska SV, Didenko GV, Potebnya GP, Bogutska KI, Prylutskyy YuI, Ritter U, Scharff P. Toxic effect of C_{60} fullerene–doxorubicin complex towards normal and tumor cells in vitro. Biopolym Cell. 2014;30:372–6.
17. Mchedlov-Petrossyan NO. Fullerenes in liquid media: an unsettling intrusion into the solution chemistry. Chem Rev. 2013; 113:5149–93.
18. Fan J, Fang G, Zeng F, Wang X, Wu S. Water-dispersible fullerene aggregates as a targeted anticancer prodrug with both chemo- and photodynamic therapeutic actions. Small. 2013;9:613–21.
19. Brant JA, Labille J, Robichaud CO, Wiesner M. Fullerol cluster formation in aqueous solution: implication for environmental release. J Colloid Interface Sci. 2007;314:281–8.
20. Zhao B, He Z, Bilski PJ, Chignell CF. Pristine (C60) and hydroxylated [C60(OH)24] fullerene phototoxicity towards HaCaT keratinocytes: Type I vs Type II mechanisms. Chem Res Toxicol. 2008;21:1056–63.
21. Ritter U, Prylutskyy YuI, Evstigneev MP, Davidenko NA, Cherepanov VV, Senenko AI, Marchenko OA, Naumovets AG. Structural features of highly stable reproducible C_{60} fullerene aqueous colloid solution probed by various techniques. Fuller Nanotub Carbon Nanostruct. 2014;23:530–4.
22. Prylutska SV, Matyshevska OV, Grynyuk II, Prylutskyy YuI, Ritter U, Scharff P. Biological effects of C_{60} fullerenes in vitro and in a model system. Mol Cryst Liq Cryst. 2007;468:265–74.
23. Prylutskyy YuI, Petrenko VI, Ivankov OI, Kyzyma OA, Bulavin LA, Litsis OO, Evstigneev MP, Cherepanov VV, Naumovets AG, Ritter U. On the origin of C_{60} fullerene solubility in aqueous solution. Langmuir. 2014;30:3967–70.
24. Song M, Liu S, Yin J, Wang H. Interaction of human serum album and C_{60} aggregates in solution. Int J Mol Sci. 2011;12:4964–74.
25. Didenko G, Prylutska S, Kichmarenko Y, Potebnya G, Prylutskyy Y, Slobodyanik N, Ritter U, Scharff P. Evaluation of the antitumor immune response to C_{60} fullerene. Mat Wiss Werkst. 2013;44:124–8.
26. Grynyuk I, Grebinyk S, Prylutska S, Mykhailova A, Franskevich D, Matyshevska O, Schutze C, Ritter U. Photoexcited fullerene C_{60} disturbs prooxidant–antioxidant balance in leukemic L1210 cells. Mat Wiss Werkst. 2013;44:139–43.
27. Ali SS, Hardt JI, Quick KL, Kim-Han JS, Erlanger BF, Huang TT, Epstein CJ, Dugan LL. A biologically effective fullerene (C60) derivative with superoxide dismutase mimetic properties. Free Radic Biol Med. 2004;37:1191–202.
28. Pani G, Bedogni B, Anzevino R, Colavitti R, Palazzotti B, Borrello S, Galeotti T. Deregulated manganese superoxide dismutase expression and resistance to oxidative injury in p53-deficient cells. Cancer Res. 2000;60:4654–60.
29. Xiong Y, Liu X, Lee CP, Chua BH, Ho YS. Attenuation of doxorubicin-induced contractile and mitochondrial dysfunction in mouse heart by cellular glutathione peroxidase. Free Radic Biol Med. 2006;41:46–55.
30. Horie M, Nishio K, Kato H, Shinohara N, Nakamura A, Fujita K, Kinugasa S, Endoh S, Yamamoto K, Yamamoto O, Niki E, Yoshida Y, Iwahashi H. In vitro evaluation of cellular responses induced by stable fullerene C_{60} medium dispersion. J Biochem. 2010;148:289–98.
31. Levi N, Hantgan R, Lively M, Carroll D, Prasad G. C_{60} Fullerenes: detection of intracellular photoluminescence and lack of cytotoxic effects. J Nanobiotechnol. 2006;4:14. doi:10.1186/1477-3155-4-14.
32. Bullard-Dillard R, Creek KE, Scrivens WA, Tour JM. Tissue sites of uptake of $^{14}C-$ labeled C_{60}. Bioorg Chem. 1996;24: 376–85.
33. Raoof M, Mackeyev Y, Cheney MA, Wilson LJ, Curley SA. Internalization of C_{60} fullerenes into cancer cells with accumulation in the nucleus via the nuclear pore complex. Biomaterials. 2012;33:2952–60.
34. Chen Ch, Xing G, Wang J, Zhao Y, Li B, Tang J, Jia G, Wang T, Sun J, Xing L, Yuan H, Gao YY, Meng H, Chen Z, Zhao F, Chai ZF, Fang X. Multihydroxylated $[Gd@C82(OH)22]_n$ nanoparticles: antineoplastic activity of high efficiency and low toxicity. Nano Lett. 2005;5:2050–7.
35. Ji Z, Sun H, Wang H, Xie Q, Liu Y, Wang Z. Biodistribution and tumor uptake of $C_{60}(OH)_x$ in mice. J Nanoparticle Res. 2006;8:53–63.
36. Rouse JG, Yang J, Barron AR, Monteiro-Riviere NA. Fullerene-based amino acid nanoparticle interactions with human epidermal keratinocytes. Toxicol In Vitro. 2006;20:1313–20.
37. Murugesan S, Mousa SA, O'Connor LJ, Lincoln DW, Linhardt RJ. Carbon inhibits vascular endothelial growth factor and fibroblast growth factor-promoted angiogenesis. FEBS Lett. 2007;581:1157–60.
38. Meng H, Xing G, Sun B, Zhao F, Lei H, Li W, Song Y, Chen Z, Yuan H, Wang X, Long J, Chen C, Liang X, Zhang N, Chai Z, Zhao Y. Potent angiogenesis inhibition by the particulate form of fullerene derivatives. ACS Nano. 2010;4:2773–83.
39. Liang XJ, Meng H, Wang Y, He H, Meng J, Lu J, Wang PC, Zhao Y, Gao X, Sun B, Chen C, Xing G, Shen D, Gottesman MM, Wu Y, Yin JJ, Jia L. Metallofullerene nanoparticles circumvent tumor resistance to cisplatin by reactivating endocytosis. Proc Natl Acad Sci USA. 2010;107:7449–54.
40. Li YY, Tian YH, Nie GJ. Antineoplastic activities of Gd@C82(OH)22 nanoparticles: tumor microenvironment regulation. Life Sci. 2012;55:884–90.